Inorganic Chemistry

pubs.acs.org/IC Article

Redox-Active Carboranyl Diphosphine as an Electron and Proton Transfer Agent

Bryce C. Nussbaum, Cameron R. Cavicchi, Mark D. Smith, Perry J. Pellechia, and Dmitry V. Peryshkov*



Cite This: https://doi.org/10.1021/acs.inorgchem.4c02022



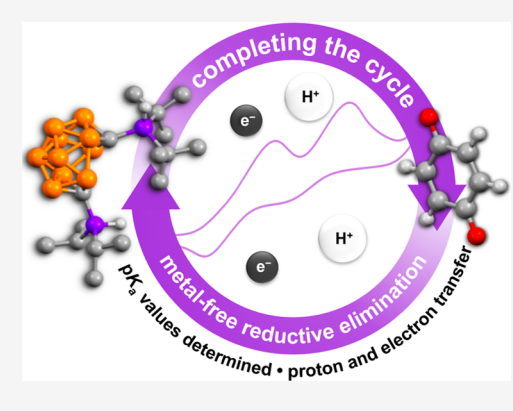
ACCESS I

Metrics & More

Article Recommendations

Supporting Information

ABSTRACT: In this work, we report the first example of the PCET reactivity for a boron cluster compound, the zwitterionic *nido*-carboranyl diphosphonium derivative $7 \cdot P(H)^t Bu_2 \cdot 10 \cdot P(H)^i Pr_2 \cdot nido \cdot C_2 B_{10} H_{10}$. This main-group reagent efficiently transfers two electrons and two protons to quinones to yield hydroquinones and regenerate a neutral *closo*-carboranyl diphosphine, $1 \cdot P^t Bu_2 \cdot 2 \cdot P^i Pr_2 \cdot closo \cdot C_2 B_{10} H_{10}$. As we have previously reported the conversion of this *closo*-carboranyl diphosphine into the zwitterionic *nido*- derivative upon reaction with main group hydrides, the transformation reported herein represents a complete synthetic cycle for the metal-free reduction of quinones, with the redoxactive carboranyl diphosphine scaffold acting as a mediator. The proposed mechanism of this reduction, based on pK_a determination, electrochemical studies, and kinetic isotope effect determination, involves the electron transfer from the *nido*- cluster to the quinone coupled with the delivery of protons.



■ INTRODUCTION

Hydrogenation reactions are important for the saturation of organic compounds, converting, for example, alkenes to alkanes, ketones to alcohols, and imines to amines. These transformations can be accomplished stoichiometrically with the use of boranes, borohydrides, aluminum hydrides, or silanes, which are highly reactive reductants with limited potential for direct recyclability. The development of organometallic chemistry introduced the use of transition metal catalysts through either direct hydrogenation with dihydrogen or transfer hydrogenation. 1-3 The activation of dihydrogen often proceeds through oxidative addition at the metal center, producing metal hydride intermediates, which in turn, formally transfer a hydride to a substrate. The classical examples of catalytically active metal complexes mainly include precious metal systems. 4-6 One of the crucial properties of these late transition metal centers is their facile two-electron cycling between oxidation states, concomitant with bond breaking and making transformations with coordinated ligands. To overcome the concerns over abundance, toxicity, cost, and functional group tolerance, organocatalytic⁷⁻¹⁰ and main group element systems have been pursued to replace or supplement transition metal catalysis. 11-15

Ambiphilic main group compounds have attracted significant attention in metallomimetic redox-active transformations. ^{16–20} Similarly to partially filled *d*-orbitals of transition metals, these systems possess empty and filled orbitals that are energetically available for breaking bonds of external substrates by simultaneous donation and acceptance of electron density. Furthermore, in a recyclable or catalytic process, bond activation represents only the first step that must be followed

by the formation and dissociation of a product, accompanied by the regeneration of an active mediator.

As a recent example, Radosevich and co-workers presented a metal-free system based on the redox cycling between phosphorus(III) and phosphorus(V). To enable this transformation, geometric constraints were enforced, altering the electronic structure of the phosphorus center in the nontrigonal phosphorus compound **A**. Reaction with ammonia borane produced dihydridophosphorane **B**, which successfully hydrogenated azobenzene, regenerating **A** (Scheme 1). A related system has been shown to engage in the oxidative addition of the C–F bonds in perfluoroarenes (Ar^F–F), ligand exchange with DIBAL-H, and reductive elimination of Ar^F–H. These findings highlight the ability of a phosphorus center to mimic transition metals in its two-electron redox cycles and perform the elementary reaction steps of a bond breaking/bond making catalytic cycle.

In addition to single-site ambiphiles, the redox behavior of metallomimetic systems can be also exhibited by larger, multicentered systems and clusters.^{23–25} We and others have been interested in the redox activity of boron clusters, which can be utilized in bond activation, electrochemical energy storage, and actinide separation.^{26–37} Carboranes are molec-

Received: May 16, 2024 **Revised:** June 27, 2024 **Accepted:** July 24, 2024



Scheme 1. Transfer Hydrogenation by a Geometrically Constrained Phosphorus Compound and a Carboranyl Diphosphine^a

Geometrically constrained phosphorus (Radosevich, 2012):

Redox-active carboranyl diphosphine (this work):

$$\begin{array}{c} P(^{\dagger}Bu)_{2} \\ \hline P(^{\dagger}Pr)_{2} \\ \hline C_{6}D_{6} \\ \hline 70 ^{\circ}C \\ \end{array} \xrightarrow{\begin{array}{c} P(^{\dagger}Pr)_{2} \\ \hline P(^{\dagger}Pr)_{2} \\ \hline \end{array}} \xrightarrow{\begin{array}{c} P(^{\dagger}Pr)_{2} \\ \hline THF \\ \hline 70 ^{\circ}C \\ \end{array}} + QF$$

^aHere, Q represents quinones in general

ular icosahedral clusters with the formula $C_2B_{10}H_{12}$ that have attracted significant attention in their organomimetic use in coordination chemistry, luminescent materials, medicinal chemistry, polymers, and batteries. These clusters feature a nonclassical, electron-deficient bonding motif, leading to extensive electron delocalization and allowing for two-electron reduction, generating dianionic *nido*-carborane structures. $^{46-50}$

We recently reported on the bond activation reactions of the carboranyl diphosphine $1-P^{t}Bu_{2}-2-P^{i}Pr_{2}-C_{2}B_{10}H_{10}$ (1). 51,52 This redox-active carborane scaffold has the ability to accept two electrons in the cluster, while the two phosphine arms act as electron-donating sites. Carboranyl disphosphine 1 was found to activate main group hydrides yielding a C_2 -symmetric reduced open nido- $\{C_2B_{10}\}^{2-}$ cluster, evidenced by the change in signal splitting from doublets to singlets in the ³¹P NMR spectra, as well as crystallographic studies. While successful oxidative addition-type reactions have been realized with our system in the reactions of 1 with main group hydrides generating the zwitterionic nido-carboranyl diphosphine 7- $P(H)^{t}Bu_{2}-10-P(H)^{i}Pr_{2}-nido-C_{2}B_{10}H_{10}$ (2), the reverse process, which would represent a closure of a synthetic cycle, remained unexplored. Herein we report the reduction of quinones by 2, which proceeds with the regeneration of the initial closocarboranyl diphosphine 1.

■ RESULTS AND DISCUSSION

First, we explored the reactivity of **2** in proton, electron, hydrogen atom, and hydride transfer reactions. The phosphonium centers in zwitterionic **2** are potentially acidic. The lability of the protons in **2** was probed by the exchange with deuterium in the presence of D_2O . An addition of D_2O (10 equiv) to a THF solution of **2** led to the emergence of two new sets of 1:1:1 triplet signals in the ³¹P NMR spectrum, indicative of ³¹P–²D coupling (${}^1J_{PD} = 68$ Hz for the $P(D)^tBu_2$ group and ${}^1J_{PD} = 67$ Hz for the $P(D)^tPr_2$ group) in the deuterated analog **2**-*d*, which were isotopically shifted from the initial signals of **2**.

Further, we found that **2** can be deprotonated in the reaction with 1,8-diazabicyclo[5.4.0]undec-7-ene (DBU), according to ³¹P NMR spectroscopy. The resonances corresponded to those of dianionic $\mathbf{1}^{2-}$, which has been previously synthesized by reduction of **1** with sodium metal. ⁵¹ We have not been able to grow single crystals of the $[DBUH^+]_2[\mathbf{1}^{2-}]$ salt yet. Instead,

during its attempted crystallization, this very air-sensitive reactive anionic species was oxidized by adventitious traces of oxygen, forming 3, which is stabilized through hydrogen bonding between the DBUH⁺ cations and phosphine oxides (Figure 1). The crystal structure of 3 retained the geometry of

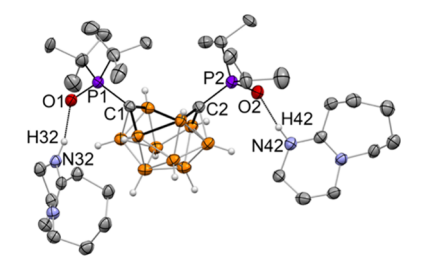


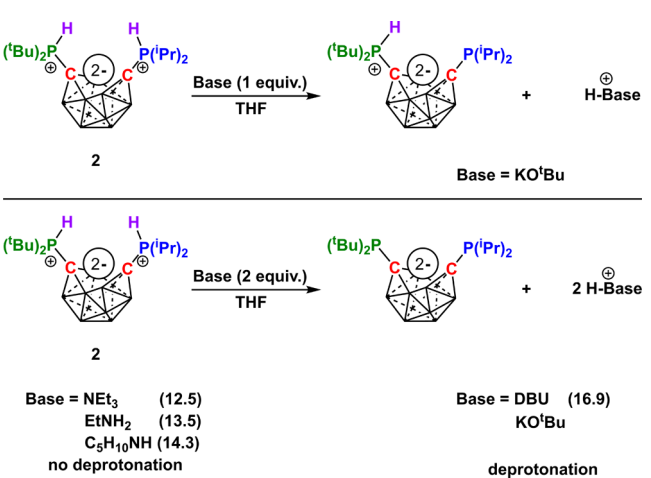
Figure 1. Displacement ellipsoid plot (50% probability) for $[DBUH]_2[7-P(O)^tBu_2-10-P(O)^tPr_2-nido-C_2B_{10}H_{10}]$, 3. Hydrogen atoms of alkyl groups and DBU cations are omitted for clarity.

the open nido- $\{C_2B_{10}\}^{2-}$ cluster. The P1–O1 and P2–O2 bonds are short (1.515(2) Å and 1.512(5) Å), representing phosphine oxide groups. The C1–P1 and C2–P2 bond lengths are shortened (1.773(3) Å and 1.763(6) Å). The DBUH⁺ cations are hydrogen bonded to oxygen atoms with N(H)···O distances of 2.664(3) Å and 2.693(3) Å and nearly linear N–H···O angles of $166(3)^{\circ}$ and $164(3)^{\circ}$. Compound 3 is related to the open phosphine oxide-decorated nido- clusters that can be obtained by chemical reduction of the corresponding closo- derivatives. ³⁶

In order to gain insight into the acidity of the P–H bonds of **2**, reactions with triethylamine, ethylamine, piperidine, and potassium *tert*-butoxide in THF were carried out. Of these, triethylamine, ethylamine, and piperidine yielded no conversion to $\mathbf{1}^{2-}$. Depending on the stoichiometry employed, the use of KO^tBu led to either single or double deprotonation of **2** indicating the closeness of its pK_{a1} and pK_{a2} values (Scheme **2**). Thus, we report that the pK_{a1} and pK_{a2} values of **2** lie between 14.3 and 16.9 in THF.

The cyclic voltammogram of **2** in THF has two partially overlapping quasi-reversible oxidation events at $E_{\rm pa}=0.01$ and 0.33 V and returning reduction events at $E_{\rm pc}=0.05$ and -0.30

Scheme 2. Reaction Scheme for 2 with Bases^a



^aThe values in parentheses are the pK_a values in THF of the conjugate acids. ⁵³

V vs $Fc^{+/0}$, suggesting that either one-electron or two-electron transformations could be possible in this system (Figure 2).

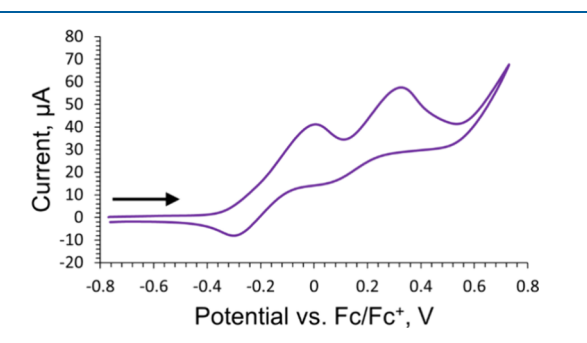
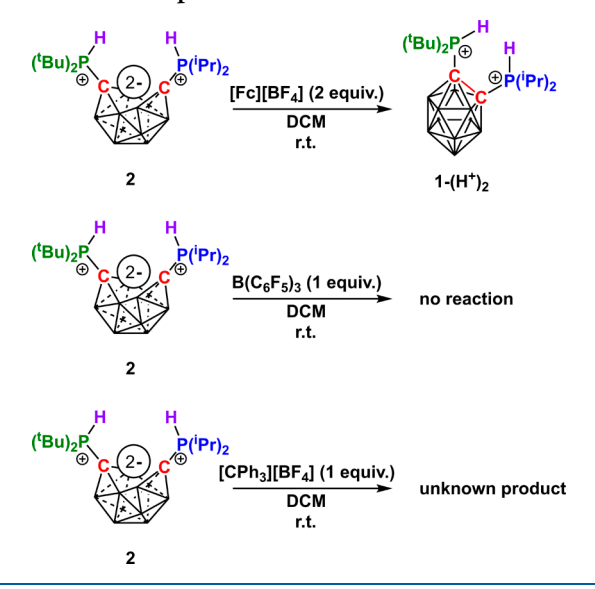


Figure 2. Cyclic voltammogram of **2** in THF. See ESI for experiment parameters.

Chemical oxidation of **2** with two equivalents of ferrocenium tetrafluoroborate ($[Fc][BF_4]$) in dichloromethane proceeded cleanly to form a *closo*- cluster product **1-(H**⁺)₂, where both phosphine groups remained protonated (Scheme 3). We

Scheme 3. Reaction Scheme for the Oxidation and Hydride Abstraction Attempts with 2



probed the acidity of the P–H bonds in this product by the addition of various weaker bases, including pyrazine (p K_a = 1.4 in THF⁵³), which deprotonated only the PⁱPr₂ group, yielding monoprotonated 1-H⁺. Interestingly, 1-H⁺ was also cleanly formed upon washing 1-(H⁺)₂ with hexanes and redissolving in diethyl ether. Removal of the remaining proton from 1-H⁺ required the addition of pyridine, a stronger base (p K_a = 5.5 in THF⁵³).

The reaction of **2** with two equivalents of TEMPO at 70 °C slowly produced a color change from red-orange to yellow. The loss of red color suggested the transformation of the radical TEMPO species into the colorless TEMPO-H. The ³¹P NMR spectrum of the reaction mixture revealed the formation of the *closo*- form **1**. This transformation suggests that hydrogen atom abstraction from **2** can occur, albeit only slowly in the case of TEMPO. A putative radical intermediate corresponding to the single hydrogen atom transfer process

could not be observed as the reaction of **2** with one equivalent of TEMPO yielded a mixture of **1** and unreacted **2**.

Addition of the trityl salt [CPh3][BF4] to 2 in dichloromethane did not lead to the expected cluster closure; instead, the ³¹P NMR spectrum of the reaction mixture featured two new sets of singlet signals, characteristic of an open nidocluster. These signals exhibited significant coupling in the proton-coupled ^{31}P NMR spectrum ($^{1}J_{PH}$ = 448 Hz for the $P^{t}Bu_{2}$ group and ${}^{1}J_{PH}$ = 465 Hz for the $P^{i}Pr_{2}$ group), indicative of the presence of P-H bonds. Notably, the reaction of 2 with one equivalent of [Fc][BF₄] produced the same set of singlets in the ³¹P NMR spectrum along with unreacted 2. Unfortunately, our attempts to obtain single crystals of these products were unsuccessful. We are willing to speculate that these products result not from direct hydride abstraction from 2, but instead are produced by one-electron transfer processes that the trityl cation is known to engage in. In the case of the reaction of 2 with [CPh₃][BF₄] in dichloromethane, the resulting solution immediately turned wine-red, with the color fading to colorless in a few days upon standing under nitrogen atmosphere. This color change prompted us to obtain the room temperature EPR spectrum of the freshly prepared winered reaction mixture, which exhibited one broadened singlet signal with g = 2.00633 (Figure S26). The absence of hyperfine coupling in the EPR spectrum suggests the localization of an unpaired electron within the boron cage.⁵⁴ No coupling to the ³¹P nucleus was observed in the EPR spectrum. The broadness of the EPR signal also prevented the observation of the trityl radical, which is another potential EPR-active component of the mixture. For the diamagnetic species present, the ³¹P and ¹¹B NMR spectra of the product indicate that the cluster is still in the open nido- form. We have previously observed the isomerization of the C_2 -symmetric nido- cluster present in 2 into a C_s-symmetric nido- cluster during oxidation attempts.⁵² The mass spectrum of the reaction mixture provided some information on the composition of the product. Two major species exhibiting isotope patterns typical for boron clusters were observed: one with smaller intensity, corresponding to the exact mass for 2, and another with larger intensity, corresponding to the loss of one BH unit from 2, thus suggesting a deboronation event. Overall, the results obtained for the reaction of 2 with the trityl cation suggest the oneelectron oxidation of 2 followed by its conversion to a diamagnetic unidentified product. The attempts to establish its structure are ongoing in our laboratory. At the same time, we found that the attempt of a hydride abstraction from 2 by $B(C_6F_5)_3$ resulted in no reaction (Scheme 3).

The density functional theory calculations of the electronic structure of 2 utilizing ADF⁵⁵ with the hybrid PBE0 functional and the TZP basis set⁵⁶ demonstrated the electron-rich nature of the open *nido*- cluster. Specifically, the HOMO of the molecule is contained within the dianionic cluster, while the LUMO spans the cluster and contains π -bonding fragments between the cage carbons and phosphorus atoms (Figure S29). Additionally, the LUMO contains lobes that are antibonding with respect to the P–H bonds. These results suggest that 2 can be considered an electron and proton donor.

Overall, these results indicate that 2 could serve as a reagent in the proton and electron transfer processes, where it would revert to 1, closing a synthetic cycle. With electrochemical data and deprotonation results in hand, we applied the Bordwell equation to estimate the bond dissociation free energy (BDFE) for the P–H bonds in 2.⁵⁷ While the reversible first reduction

Table 1. Conversion of 2 and Quinones to 1 and Hydroquinones

General scheme	('Bu) ₂ P (Pr) ₂ + Q THF 1 d 70 °C 1					
Quinones	structure	°	NC CN			
	name	<i>para</i> - benzoquinone	tetracyanoquino dimethane	9,10- phenanthrene quinone	2-methyl-1,4- naphthoquinone	anthraquinone
Conversion	31P NMRa	100	80 ^b	100	100	20
	¹³ C NMR	100	_b	100	100	n.d.c

[&]quot;Conversion is determined by the ratio in integrations between products and 2. "TCNQ was reduced at room temperature. Upon heating, TCNQ reacts with 1 as it is formed, leading to a plateau in the conversion of 2 (see Figure S27). Due to poor solubility, conversion of anthraquinone could not be observed by ¹³C NMR spectroscopy.

Scheme 4. Reaction Scheme for 2 with para-Benzoquinone

^aYields shown for the phosphorus-containing products were determined by ³¹P NMR spectroscopy

potential for the 2/1- $(H^+)_2$ couple could not be obtained from cyclic voltammetry experiments in THF, which produced quasi-reversible traces, the use of a midpoint between peak $E_{\rm pa}$ and $E_{\rm pc}$ values can serve to estimate E_1 as 0.14 V. The deprotonation of 1- $(H^+)_2$ by pyrazine in THF (p K_a = 1.4 in THF⁵³) can serve to approximate the upper boundary for its p K_{a1} value. Understanding the limitations in the available data, the estimate for BDFE(P–H) for 2 was obtained using the Bordwell equation ($C_{\rm G(THF)}$ = 59.9 kcal/mol) as 65 kcal/mol. This value places 2 close to TEMPO-H (65.5 kcal/mol in THF) and lower than hydroquinone (67.2 kcal/mol in THF). The closeness of the BDFE values for 2 and TEMPO-H may explain the slow reaction of 2 and TEMPO described above.

Thus, we experimentally probed the reduction capability of 2 in the reactions with quinones. Quinones are known for their propensity to engage in PCET reactions, accepting two electrons paired with the acceptance of two protons. ^{59,60} In addition, the change in the carbonyl carbon atom character can be easily monitored by ¹³C NMR spectroscopy.

The results of the reduction experiments are summarized in Table 1. The reaction of 2 with one equivalent of 9,10-phenanthrenequinone yielded 1 and 9,10-phenanthrenediol after 30 min at 70 °C, cleanly producing the characteristic set of doublets for 1 in the ³¹P NMR spectrum and showing the loss of the carbonyl carbon resonance in the ¹³C NMR spectrum. High conversions were also observed upon reaction of 2 with *para*-benzoquinone, 2-methyl-1,4-naphthoquinone, and the related tetracyanoquinodimethane (TCNQ).

While 2 rapidly converted to 1 in the reactions with quinones at 70 °C, the elevated temperature was not required for select quinones. For example, *para*-benzoquinone reacted with 2 upon mixing at room temperature and consistently

produced 1 and a new open cage *nido*- product 4 in an 8.3:1 ratio (Scheme 4). The new product was isolated and characterized by single crystal X-ray crystallography and features an activated hydroquinone bridging the two phosphonium centers on the *nido*-carboranyl backbone (Figure 3). Additionally, the reaction of 2 with TCNQ cleanly

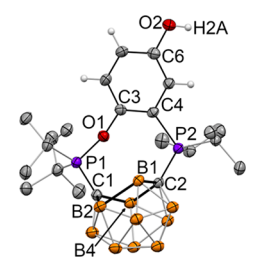


Figure 3. Displacement ellipsoid plot (50% probability) for 4. Hydrogen atoms of alkyl groups and the carborane cluster are omitted for clarity.

proceeded at room temperature to form $TCNQH_2$ and regenerate 1, while the reaction at 70 $^{\circ}C$ led to the formation of additional unidentified products.

Notably, 4 is not based on the same C_2 -symmetric *nido*-cluster that the starting 2 contains. Instead, a *nido*-1,3- $\{C_2B_{10}\}^{2-}$ isomer is formed, where the open face of the cluster is a highly distorted five-membered C_2B_3 ring with an elongated B1–B2 bond (1.928(4) Å).⁵⁰ In this cluster isomer, the C1 carbon atom is tetrahedral, while the C2 carbon atom is five-coordinate in a distorted square-pyramid environment. The change of the geometry of the cluster in this reaction indicates the occurrence of the cage-closing and reopening redox sequence en route to 4 and the enforcement of the

smaller cage opening size due to the quinone fragment bridging the two phosphorus centers.

The C1–P1 and C2–P2 bonds in 4 are shortened (1.713(2) Å and 1.765(2) Å, respectively), which indicates their partial ylide character. The P1–O1 bond length is 1.619(2) Å. The C3–O1(P1) bond (1.398(3) Å) is longer than the C6–O2(H2A) bond (1.373(3) Å). The structure of 4 can be considered a unique amalgamation of two separate pathways for the reaction of *para*-benzoquinones and phosphines: a 1,4-addition product with the newly formed C–P bond and the Schönberg-type adduct with the P–O bond. Normally, the 1,4-addition product forms in the reaction of *para*-benzoquinone and triarylphosphines.⁶¹

The details of the mechanistic steps leading to the formation of the minor product 4 are unclear at the moment. As mentioned above, the change in the reduced cluster geometry may indicate an oxidation step that initially leads to its closure. At the same time, we found that the parent *closo-* cluster 1 does not react with benzoquinone under these conditions. Furthermore, neither 1 nor 2 reacts with hydroquinone to produce 4.

The experiments with anthraquinone proved difficult in the characterization of the reduced product and quantification of the conversion, due to the relatively poor solubility in THF. Conversion of 2 to 1 was observable in ³¹P NMR spectra, but ¹³C NMR spectra did not provide useful resonances to confirm the changes to the quinone structure.

Select diketones have also been shown to react with 2. For example, diphenylethanedione (commonly called benzil) converted 2 back to 1, producing the diol product (10% conversion). However, simple alkyl- or aryl-substituted ketones resisted the reduction by our system. Thus far, acetone, benzophenone, acetophenone, valerophenone, and chalcone afforded only negligible yields of 1.

A 40:60 mixture of **2** and **2**-*d*, obtained in the isotope exchange with D_2O described above, demonstrated clean conversion to **1** in the reaction with 2-methyl-1,4-naphthoquinone at 70 °C (Figure S28). The comparative rates of consumption for **2** and **2**-*d* were found to be close to each other, representing a primary isotope effect k(H)/k(D) of 1.02. The absence of a significant KIE renders the initial proton transfer or homolytic cleavage of P–H bonds in **2** an unlikely step in the reaction with quinones while not completely ruling out a concerted EPT process. 62,63

The transformations described above lead us to propose a mechanism for the reduction of quinones by 2 wherein the electron transfers are associated with proton transfers. As we demonstrated, the relatively high pK_a of the P-H bonds in 2 likely precludes the initial deprotonation by quinones, for which the initial protonation is generally unfavorable. The absence of a significant primary KIE for P-H/D bonds corroborates this conjecture. At the same time, the oxidation of 2 readily produces $1-(H^+)_2$, which is significantly more acidic due to the loss of zwitterion stabilization, thus suggesting a possibility for a PCET process. Considering the quinones used in this work, the involvement of protons is important for the observed reactivity. For example, the 2 $e^{-}/2$ H⁺ reduction potential for benzoquinone is significantly positive (E = 0.643V vs NHE), while the electron-only 1 e^- reduction of benzoquinone ($E = -0.882 \text{ V vs } \text{Fc/Fc}^+$) is unlikely to be favorable with 2, as it is not a strong reductant.⁶⁴ The importance for proton-quinone interactions, including hydrogen bonding, has been recognized as a factor governing reduction potentials.⁶⁰ The somewhat slow rates of the reactions of **2** with quinones and TEMPO may be a consequence of significant structural rearrangements that accompany its transformation from the nido-{ C_2B_{10} } 2 to the closo-{ C_2B_{10} } cluster.

CONCLUSIONS

In conclusion, we demonstrated the PCET reactivity of the zwitterionic *nido*-carboranyl diphosphonium 2 in the reduction of quinones with the formation of the closed, neutral diphosphine 1. This transformation represents a closure of a synthetic cycle for metal-free quinone reduction, featuring a redox-active carboranyl diphosphine as a mediator. The proposed mechanism involves the delivery of electrons and protons from the reduced form 2 to electrophilic substrates. As the starting diphosphine 1 can be reconverted into 2 upon reaction with main group hydrides, we anticipate that further efforts will likely lead to the implementation of carborane cluster compounds in one-pot catalytic reductive transformations.

■ EXPERIMENTAL SECTION

All synthetic manipulations, unless stated otherwise, were carried out in a nitrogen-filled VAC glovebox. The solvents were sparged with nitrogen, passed through activated alumina, and stored over activated 4 Å Linde-type molecular sieves. Benzene- d_6 was degassed and stored over activated 4 Å Linde-type molecular sieves. NMR spectra were recorded using Varian spectrometers at 400 ($^1\mathrm{H}$) and 100 ($^{13}\mathrm{C}$) MHz, reported in δ (parts per million), and referenced to the residual $^1\mathrm{H}/^{13}\mathrm{C}$ signals of the deuterated solvent. J values are given in Hz.

ortho-Carborane ($C_2B_{10}H_{12}$, Boron Specialties), tributylstannane (Bu_3SnH , 97%, Acros Organics), and the other chemicals were used as received. No uncommon hazards are noted.

Synthesis of 7-P(H)^tBu₂-10-P(H)^tPr₂-nido-C₂B₁₀H₁₀ (2). The synthesis followed a modified literature procedure. A sample of 1-P^tBu₂-2-P^tPr₂-closo-C₂B₁₀H₁₀ (1) (100 mg, 0.247 mmol), was dissolved in 2.00 mL of benzene-d₆. To the vial was added a portion of tributylstannane (0.140 mL, 0.520 mmol, 2.11 equiv). The yellow solution was heated at 70 °C for 4 days, at which point colorless crystals had precipitated out. The solution was drawn up, and the crystals were washed with hexanes (3 \times 2 mL). The NMR signals were identical to those previously reported.

Reaction of 2 with Deuterium Oxide. A 0.500 mL aliquot of a 0.0902 M solution of **2** in THF (0.0451 mmol) was added to an NMR tube. On the benchtop, a portion of deuterium oxide (8.16 μ L, 0.4510 mmol, 10.0 equiv) was added to the NMR tube, which was placed in a 70 °C oil bath for 1 day. The solution was subsequently washed with hexanes (2 × 2 mL). The conversion was monitored by ³¹P NMR spectroscopy.

Reaction of 2 with Potassium *tert*-Butoxide (1 equiv). A 0.500 mL aliquot of a 0.0701 M solution of 2 in THF (0.0351 mmol) was added to a vial containing potassium *tert*-butoxide (4 mg, 0.0356 mmol, 1.02 equiv). The solution immediately became yellow. The conversion was monitored by ³¹P and ¹¹B NMR spectroscopies.

Reaction of 2 with Potassium *tert*-Butoxide (≥2 equiv). A 0.500 mL aliquot of a 0.0853 M solution of 2 in THF (0.0426 mmol) was added to a vial containing potassium *tert*-butoxide (12 mg, 0.107 mmol, 2.51 equiv). The solution immediately became orange. The conversion was monitored by ³¹P and ¹¹B NMR spectroscopies.

Reaction of 2 with 1,8-Diazabicyclo[5.4.0]undec-7-ene (DBU). To a 0.500 mL aliquot of a 0.0836 M solution of 2 in THF (0.0418 mmol) was added a portion of DBU (15.7 μL, 0.1050 mmol, 2.51 equiv). The conversion was monitored by ³¹P NMR spectroscopy. Colorless single crystals were grown from the slow evaporation of a hexanes/DCM mixed solvent system.

Reaction of 2 with Ferrocenium Tetrafluoroborate. A 0.380 mL aliquot of a 0.1019 M solution of 2 in DCM (0.0387 mmol) was

added to a vial containing ferrocenium tetrafluoroborate (21 mg, 0.0770 mmol, 1.99 equiv), prepared according to literature. The dark green solution was stirred at room temperature for 1 h. Volatiles were removed *in vacuo*, and the solid was washed with 0.500 mL of hexanes before being redissolved in diethyl ether, producing a yellow solution of 1-H⁺ and ferrocene. The remaining impurities and 1-(H⁺)₂ were found to be soluble in DCM and acetonitrile. The conversion was monitored by ^{31}P and ^{11}B NMR spectroscopies.

Reaction of 2 with (2,2,6,6-Tetramethylpiperidin-1-yl)oxyl (TEMPO) (1 equiv). A 0.500 mL aliquot of a 0.0701 M solution of 2 in THF (0.0351 mmol) was added to a vial containing TEMPO (6 mg, 0.0384 mmol, 1.10 equiv). The pink solution was transferred to an NMR tube, which was placed in a 70 °C oil bath for 1 day. The conversion was monitored by ³¹P NMR spectroscopy.

Reaction of 2 with TEMPO (2 equiv). A 0.500 mL aliquot of a 0.0902 M solution of **2** in THF (0.0451 mmol) was added to a vial containing TEMPO (14 mg, 0.0896 mmol, 1.99 equiv). The solution was transferred to an NMR tube, which was placed in a 70 $^{\circ}$ C oil bath for 3 days. Over the course of the reaction, the color of the solution turned from red-orange to yellow. Volatiles were removed *in vacuo*, and the solid was washed with hexanes (2 × 4 mL) to extract **1**. The conversion was monitored by 31 P and 11 B NMR spectroscopies.

Reaction of 2 with Triphenylcarbenium Tetrafluoroborate. To a 1.00 mL aliquot of a 0.0615 M solution of 2 in DCM (0.0615 mmol) was added a sample of triphenylcarbenium tetrafluoroborate (20 mg, 0.0606 mmol, 0.985 equiv) dissolved in 1.00 mL of DCM. Immediately upon addition, the solution turned wine-red. The conversion was monitored by ³¹P, ¹¹B, and ¹³C NMR and EPR spectroscopies and mass spectrometry.

Reaction of 2 with *para*-Benzoquinone. A 0.450 mL aliquot of a 0.1021 M solution of 2 in THF (0.0459 mmol) was added to a vial containing crystalline *para*-benzoquinone (5 mg, 0.0463 mmol, 1.01 equiv). The solution was left to sit for 3 days at room temperature. Volatiles were removed *in vacuo*, and the resulting solid was washed with hexanes. Colorless single crystals were grown from the slow evaporation of DCM. The conversion was monitored by ³¹P and ¹³C NMR spectroscopies.

Reaction of 2 with Tetracyanoquinodimethane (TCNQ). Outside of the glovebox, a 0.500 mL aliquot of a 0.0947 M solution of 2 in THF (0.0473 mmol) was added to a vial containing TCNQ (10 mg, 0.0490 mmol, 1.03 equiv). The solution immediately turned neon green and was stirred at room temperature for 4 h. The conversion was monitored by $^{\rm 31}P$ and $^{\rm 13}C$ NMR spectroscopies.

Reaction of 2 with 9,10-Phenanthrenequinone. A $0.500~\mathrm{mL}$ aliquot of a $0.100~\mathrm{M}$ solution of 2 in THF ($0.0500~\mathrm{mmol}$) was added to a vial containing 9,10-phenanthrenequinone ($11~\mathrm{mg}$, $0.0528~\mathrm{mmol}$, $1.06~\mathrm{equiv}$). The solution was transferred to an NMR tube, which was placed in a $70~\mathrm{^{\circ}C}$ oil bath for 30 min. The conversion was monitored by $^{31}\mathrm{P}$ and $^{13}\mathrm{C}$ NMR spectroscopies.

Reaction of 2 with 2-Methyl-1,4-naphthoquinone. A 0.500 mL aliquot of a 0.113 M solution of 2 in THF (0.0566 mmol) was added to a vial containing 2-methyl-1,4-naphthoquinone (10 mg, 0.0581 mmol, 1.03 equiv). The solution was transferred to an NMR tube, which was placed in a 70 $^{\circ}$ C oil bath for 8 h. The conversion was monitored by 31 P and 13 C NMR spectroscopies.

Reaction of 2 with Anthraquinone. A 0.500 mL aliquot of a 0.0945 M solution of **2** in THF (0.0472 mmol) was added to a vial containing anthraquinone (10 mg, 0.0480 mmol, 1.02 equiv). The mixture was transferred to an NMR tube, which was placed in a 70 $^{\circ}$ C oil bath for 8 days. During this time, the relatively insoluble anthraquinone appeared to sublime and deposit at the bottom of the NMR tube as yellow crystals. The conversion was monitored by 31 P and 13 C NMR spectroscopies.

Reaction of 2 with Diphenylethanedione (Benzil). A 0.500 mL aliquot of a 0.0902 M solution of 2 in THF (0.0451 mmol) was added to a vial containing benzil (19 mg, 0.0904 mmol, 2.00 equiv) and an internal standard (1,3,5-trimethoxybenzene, 8 mg, 0.0476 mmol, 1.05 equiv) dissolved in 1 mL of THF. The solution was stirred at room temperature for 1 h and was concentrated to 0.500 mL in vacuo. The solution was transferred to an NMR tube, which was

placed in a 70 $^{\circ}$ C oil bath for 2 days. The conversion was monitored by 31 P, 13 C, and 1 H NMR spectroscopies.

ASSOCIATED CONTENT

Supporting Information

The Supporting Information is available free of charge at https://pubs.acs.org/doi/10.1021/acs.inorgchem.4c02022.

Crystallography details, NMR and EPR spectra, electrochemistry parameters, and DFT calculations (PDF)

Accession Codes

CCDC 2347041–2347042 contain the supplementary crystallographic data for this paper. These data can be obtained free of charge via www.ccdc.cam.ac.uk/data_request/cif, or by emailing data_request/cif, or by contacting The Cambridge Crystallographic Data Centre, 12 Union Road, Cambridge CB2 1EZ, UK; fax: +44 1223 336033.

AUTHOR INFORMATION

Corresponding Author

Dmitry V. Peryshkov — Department of Chemistry and Biochemistry, University of South Carolina, Columbia, South Carolina 29208, United States; orcid.org/0000-0002-5653-9502; Email: peryshkov@sc.edu

Authors

Bryce C. Nussbaum – Department of Chemistry and Biochemistry, University of South Carolina, Columbia, South Carolina 29208, United States

Cameron R. Cavicchi – Department of Chemistry and Biochemistry, University of South Carolina, Columbia, South Carolina 29208, United States

Mark D. Smith – Department of Chemistry and Biochemistry, University of South Carolina, Columbia, South Carolina 29208, United States

Perry J. Pellechia – Department of Chemistry and Biochemistry, University of South Carolina, Columbia, South Carolina 29208, United States

Complete contact information is available at: https://pubs.acs.org/10.1021/acs.inorgchem.4c02022

Notes

The authors declare no competing financial interest.

ACKNOWLEDGMENTS

This material is based in part upon work supported by the National Science Foundation under Award CHE-2154828. We are grateful to the Advanced Support for Innovative Research Excellence program of the Office of the Vice President for Research at the University of South Carolina.

■ REFERENCES

- (1) Noyori, R.; Ohkuma, T. Asymmetric Catalysis by Architectural and Functional Molecular Engineering: Practical Chemo- and Stereoselective Hydrogenation of Ketones. *Angew. Chem., Int. Ed.* **2001**, *40* (1), 40–73.
- (2) Ikariya, T.; Murata, K.; Noyori, R. Bifunctional Transition Metal-Based Molecular Catalysts for Asymmetric Syntheses. *Org. Biomol. Chem.* **2006**, *4* (3), 393–406.
- (3) Abdur-Rashid, K.; Lough, A. J.; Morris, R. H. Ruthenium Dihydride RuH₂(PPh₃)₂((R,R)-Cyclohexyldiamine) and Ruthenium Monohydride RuHCl(PPh₃)₂((R,R)-Cyclohexyldiamine): Active Catalyst and Catalyst Precursor for the Hydrogenation of Ketones and Imines. *Organometallics* **2000**, *19* (14), 2655–2657.

- (4) Shvo, Y.; Czarkie, D.; Rahamim, Y.; Chodosh, D. F. A New Group of Ruthenium Complexes: Structure and Catalysis. *J. Am. Chem. Soc.* **1986**, *108* (23), 7400–7402.
- (5) Osborn, J. A.; Jardine, F. H.; Young, J. F.; Wilkinson, G. The Preparation and Properties of Tris(Triphenylphosphine)-Halogenorhodium(I) and Some Reactions Thereof Including Catalytic Homogeneous Hydrogenation of Olefins and Acetylenes and Their Derivatives. J. Chem. Soc. Inorg. Phys. Theor. 1966, 0, 1711–1732.
- (6) Crabtree, R. Iridium Compounds in Catalysis. Acc. Chem. Res. 1979, 12 (9), 331–337.
- (7) Adolfsson, H. Organocatalytic Hydride Transfers: A New Concept in Asymmetric Hydrogenations. *Angew. Chem., Int. Ed.* **2005**, 44 (22), 3340–3342.
- (8) Dalko, P. I.; Moisan, L. In the Golden Age of Organocatalysis. *Angew. Chem., Int. Ed.* **2004**, 43 (39), 5138–5175.
- (9) MacMillan, D. W. C. The Advent and Development of Organocatalysis. *Nature* **2008**, 455 (7211), 304–308.
- (10) Huang, Y.; Walji, A. M.; Larsen, C. H.; MacMillan, D. W. C. Enantioselective Organo-Cascade Catalysis. *J. Am. Chem. Soc.* **2005**, 127 (43), 15051–15053.
- (11) Chase, P. A.; Welch, G. C.; Jurca, T.; Stephan, D. W. Metal-Free Catalytic Hydrogenation. *Angew. Chem., Int. Ed.* **2007**, 46 (42), 8050–8053.
- (12) Stephan, D. W.; Greenberg, S.; Graham, T. W.; Chase, P.; Hastie, J. J.; Geier, S. J.; Farrell, J. M.; Brown, C. C.; Heiden, Z. M.; Welch, G. C.; Ullrich, M. Metal-Free Catalytic Hydrogenation of Polar Substrates by Frustrated Lewis Pairs. *Inorg. Chem.* **2011**, *50* (24), 12338–12348.
- (13) Légaré, M.-A.; Pranckevicius, C.; Braunschweig, H. Metallomimetic Chemistry of Boron. *Chem. Rev.* **2019**, *119* (14), 8231–8261
- (14) Frey, G. D.; Lavallo, V.; Donnadieu, B.; Schoeller, W. W.; Bertrand, G. Facile Splitting of Hydrogen and Ammonia by Nucleophilic Activation at a Single Carbon Center. *Science* **2007**, *316* (5823), 439–441.
- (15) Frey, G. D.; Masuda, J. D.; Donnadieu, B.; Bertrand, G. Activation of Si-H, B-H, and P-H Bonds at a Single Nonmetal Center. *Angew. Chem., Int. Ed.* **2010**, 49 (49), 9444–9447.
- (16) Chu, T.; Nikonov, G. I. Oxidative Addition and Reductive Elimination at Main-Group Element Centers. *Chem. Rev.* **2018**, *118* (7), 3608–3680.
- (17) Lipshultz, J. M.; Li, G.; Radosevich, A. T. Main Group Redox Catalysis of Organopnictogens: Vertical Periodic Trends and Emerging Opportunities in Group 15. J. Am. Chem. Soc. 2021, 143 (4), 1699–1721.
- (18) Weetman, C.; Inoue, S. The Road Travelled: After Main-Group Elements as Transition Metals. *ChemCatChem.* **2018**, *10* (19), 4213–4228
- (19) Bonfante, S.; Lorber, C.; Lynam, J. M.; Simonneau, A.; Slattery, J. M. Metallomimetic C-F Activation Catalysis by Simple Phosphines. J. Am. Chem. Soc. 2024, 146 (3), 2005–2014.
- (20) Abbenseth, J.; Goicoechea, J. M. Recent Developments in the Chemistry of Non-Trigonal Pnictogen Pincer Compounds: From Bonding to Catalysis. *Chem. Sci.* **2020**, *11* (36), 9728–9740.
- (21) Dunn, N. L.; Ha, M.; Radosevich, A. T. Main Group Redox Catalysis: Reversible PIII/PV Redox Cycling at a Phosphorus Platform. J. Am. Chem. Soc. 2012, 134 (28), 11330–11333.
- (22) Lim, S.; Radosevich, A. T. Round-Trip Oxidative Addition, Ligand Metathesis, and Reductive Elimination in a PIII/PV Synthetic Cycle. J. Am. Chem. Soc. 2020, 142 (38), 16188–16193.
- (23) Power, P. P. Interaction of Multiple Bonded and Unsaturated Heavier Main Group Compounds with Hydrogen, Ammonia, Olefins, and Related Molecules. *Acc. Chem. Res.* **2011**, 44 (8), 627–637.
- (24) Tsukahara, N.; Asakawa, H.; Lee, K.-H.; Lin, Z.; Yamashita, M. Cleaving Dihydrogen with Tetra(o-Tolyl)Diborane(4). *J. Am. Chem. Soc.* **2017**, *139* (7), 2593–2596.
- (25) Su, Y.; Kinjo, R. Small Molecule Activation by Boron-Containing Heterocycles. *Chem. Soc. Rev.* **2019**, 48 (13), 3613–3659.

- (26) Charmant, J. P. H.; Haddow, M. F.; Mistry, R.; Norman, N. C.; Orpen, A. G.; Pringle, P. G. A Simple Entry into nido- C_2B_{10} clusters: HCl Promoted Cleavage of the C–C Bond in Ortho-Carboranyl Diphosphines. *Dalton Trans.* **2008**, *11*, 1409–1411.
- (27) Schulz, J.; Kreienbrink, A.; Coburger, P.; Schwarze, B.; Grell, T.; Lönnecke, P.; Hey-Hawkins, E. 12-Vertex Zwitterionic Bis-Phosphonium-Nido-Carborates through Ring-Opening Reactions of 1,2-Diphosphetanes. *Chem. Eur. J.* **2018**, 24 (23), 6208–6216.
- (28) Wong, Y. O.; Smith, M. D.; Peryshkov, D. V. Reversible Water Activation Driven by Contraction and Expansion of a 12-Vertex-closo-12-Vertex-nido Biscarborane Cluster. *Chem. Commun.* **2016**, *52* (86), 12710–12713.
- (29) Wong, Y. O.; Smith, M. D.; Peryshkov, D. V. Synthesis of the First Example of the 12-Vertex-closo/12-Vertex-nido Biscarborane Cluster by a Metal-Free B—H Activation at a Phosphorus(III) Center. *Chem. Eur. J.* **2016**, 22 (20), 6764–6767.
- (30) Nussbaum, B. C.; Humphries, A. L.; Gange, G. B.; Peryshkov, D. V. Redox-Active Carborane Clusters in Bond Activation Chemistry and Ligand Design. *Chem. Commun.* **2023**, *59* (66), 9918–9928.
- (31) Wang, H.; Zhang, J.; Lee, H. K.; Xie, Z. Borylene Insertion into Cage B—H Bond: A Route to Electron-Precise B—B Single Bond. J. Am. Chem. Soc. 2018, 140 (11), 3888–3891.
- (32) Barton, J. L.; Wixtrom, A. I.; Kowalski, J. A.; Qian, E. A.; Jung, D.; Brushett, F. R.; Spokoyny, A. M. Perfunctionalized Dodecaborate Clusters as Stable Metal-Free Active Materials for Charge Storage. *ACS Appl. Energy Mater.* **2019**, 2 (7), 4907–4913.
- (33) Ready, A. D.; Irshad, A.; Kallistova, A.; Carrillo, M.; Gembicky, M.; Seshadri, R.; Narayan, S.; Spokoyny, A. M. Electrochemical Cycling of Redox-Active Boron Cluster-Based Materials in the Solid State. *J. Am. Chem. Soc.* **2023**, *145* (26), 14345–14353.
- (34) Yao, S.; Szilvási, T.; Xiong, Y.; Lorent, C.; Ruzicka, A.; Driess, M. Bis(Silylene)-Stabilized Monovalent Nitrogen Complexes. *Angew. Chem., Int. Ed.* **2020**, 59 (49), 22043–22047.
- (35) Yao, S.; Kostenko, A.; Xiong, Y.; Ruzicka, A.; Driess, M. Redox Noninnocent Monoatomic Silicon(0) Complex ("Silylone"): Its One-Electron-Reduction Induces an Intramolecular One-Electron-Oxidation of Silicon(0) to Silicon(I). *J. Am. Chem. Soc.* **2020**, *142* (29), 12608–12612.
- (36) Keener, M.; Mattejat, M.; Zheng, S.-L.; Wu, G.; Hayton, T. W.; Ménard, G. Selective Electrochemical Capture and Release of Uranyl from Aqueous Alkali, Lanthanide, and Actinide Mixtures Using Redox-Switchable Carboranes. *Chem. Sci.* **2022**, *13* (12), 3369–3374.
- (37) Ready, A. D.; Nelson, Y. A.; Torres Pomares, D. F.; Spokoyny, A. M. Redox-Active Boron Clusters. *Acc. Chem. Res.* **2024**. 571310.
- (38) Grimes, R. N. Carboranes, Third ed.; Academic Press: Amersterdam; Boston, 2016.
- (39) Grimes, R. N. Carboranes in the Chemist's Toolbox. *Dalton Trans.* **2015**, 44 (13), 5939–5956.
- (40) Hawthorne, M. F. Boranes and Beyond: History and the Man Who Created Them; Springer: New York, NY, 2023. .
- (41) Tomich, A. W.; Chen, J.; Carta, V.; Guo, J.; Lavallo, V. Electrolyte Engineering with Carboranes for Next-Generation Mg Batteries. ACS Cent. Sci. 2024, 10 (2), 264–271.
- (42) Zhang, X.; Rendina, L. M.; Müllner, M. Carborane-Containing Polymers: Synthesis, Properties, and Applications. *ACS Polym. Au* **2024**, *4* (1), 7–33.
- (43) Stockmann, P.; Gozzi, M.; Kuhnert, R.; Sárosi, M. B.; Hey-Hawkins, E. New Keys for Old Locks: Carborane-Containing Drugs as Platforms for Mechanism-Based Therapies. *Chem. Soc. Rev.* **2019**, 48 (13), 3497–3512.
- (44) Qiu, Z.; Xie, Z. Functionalization of o-Carboranes via Carboryne Intermediates. *Chem. Soc. Rev.* **2022**, *51* (8), 3164–3180.
- (45) Grams, R. J.; Santos, W. L.; Scorei, I. R.; Abad-García, A.; Rosenblum, C. A.; Bita, A.; Cerecetto, H.; Viñas, C.; Soriano-Ursúa, M. A. The Rise of Boron-Containing Compounds: Advancements in Synthesis, Medicinal Chemistry, and Emerging Pharmacology. *Chem. Rev.* 2024, 124 (5), 2441–2511.
- (46) Dunks, G. B.; Wiersema, R. J.; Hawthorne, M. F. Chemical and Structural Studies of the Dodecahydrodicarba-Closo-Dodecarborate-

- (2-) Ions Produced from Icosahedral Dicarbacloso-Dodecarborane(12). J. Am. Chem. Soc. 1973, 95 (10), 3174-3179.
- (47) Núñez, R.; Tarrés, M.; Ferrer-Ugalde, A.; de Biani, F. F.; Teixidor, F. Electrochemistry and Photoluminescence of Icosahedral Carboranes, Boranes, Metallacarboranes, and Their Derivatives. *Chem. Rev.* **2016**, *116* (23), 14307–14378.
- (48) Miller, J. R.; Cook, A. R.; Šimková, L.; Pospíšil, L.; Ludvík, J.; Michl, J. The Impact of Huge Structural Changes on Electron Transfer and Measurement of Redox Potentials: Reduction of Ortho-12-Carborane. *J. Phys. Chem. B* **2019**, *123* (45), 9668–9676.
- (49) McKay, D.; Macgregor, S. A.; Welch, A. J. Isomerisation of nido- $[C_2B_{10}H_{12}]^{2-}$ Dianions: Unprecedented Rearrangements and New Structural Motifs in Carborane Cluster Chemistry. *Chem. Sci.* **2015**, *6* (5), 3117–3128.
- (50) Deng, L.; Cheung, M.-S.; Chan, H.-S.; Xie, Z. Reduction of 1,2- $(CH_2)_n$ -1,2- $C_2B_{10}H_{10}$ by Group 1 Metals. Effects of Bridge Length/Rigidity on the Formation of Carborane Anions. *Organometallics* **2005**, 24 (25), 6244–6249.
- (51) Gange, G. B.; Humphries, A. L.; Royzman, D. E.; Smith, M. D.; Peryshkov, D. V. Metal-Free Bond Activation by Carboranyl Diphosphines. J. Am. Chem. Soc. 2021, 143 (29), 10842–10846.
- (52) Gange, G. B.; Humphries, A. L.; Smith, M. D.; Peryshkov, D. V. Activation of Alkynes by a Redox-Active Carboranyl Diphosphine and Formation of Boron-Containing Phosphacycles. *Inorg. Chem.* **2022**, *61* (46), 18568–18573.
- (53) Tshepelevitsh, S.; Kütt, A.; Lõkov, M.; Kaljurand, I.; Saame, J.; Heering, A.; Plieger, P. G.; Vianello, R.; Leito, I. On the Basicity of Organic Bases in Different Media. *Eur. J. Org. Chem.* **2019**, 2019 (40), 6735–6748.
- (54) Fox, M. A.; Nervi, C.; Crivello, A.; Low, P. J. Carborane Radical Anions: Spectroscopic and Electronic Properties of a Carborane Radical Anion with a 2n + 3 Skeletal Electron Count. *Chem. Commun.* **2007**, 23, 2372–2374.
- (55) te Velde, G.; Bickelhaupt, F. M.; Baerends, E. J.; Fonseca Guerra, C.; van Gisbergen, S. J. A.; Snijders, J. G.; Ziegler, T. Chemistry with ADF. *J. Comput. Chem.* **2001**, 22 (9), 931–967.
- (56) Van Lenthe, E.; Baerends, E. J. Optimized Slater-Type Basis Sets for the Elements 1–118. *J. Comput. Chem.* **2003**, 24 (9), 1142–1156.
- (57) Bordwell, F. G.; Cheng, J. P.; Harrelson, J. A. Homolytic Bond Dissociation Energies in Solution from Equilibrium Acidity and Electrochemical Data. *J. Am. Chem. Soc.* **1988**, *110* (4), 1229–1231.
- (58) Agarwal, R. G.; Coste, S. C.; Groff, B. D.; Heuer, A. M.; Noh, H.; Parada, G. A.; Wise, C. F.; Nichols, E. M.; Warren, J. J.; Mayer, J. M. Free Energies of Proton-Coupled Electron Transfer Reagents and Their Applications. *Chem. Rev.* **2022**, *122* (1), 1–49.
- (59) Guo, X.; Zipse, H.; Mayr, H. Mechanisms of Hydride Abstractions by Quinones. J. Am. Chem. Soc. 2014, 136 (39), 13863–13873.
- (60) Shi, R. R. S.; Tessensohn, M. E.; Lauw, S. J. L.; Foo, N. A. B. Y.; Webster, R. D. Tuning the Reduction Potential of Quinones by Controlling the Effects of Hydrogen Bonding, Protonation and Proton-Coupled Electron Transfer Reactions. *Chem. Commun.* **2019**, 55 (16), 2277–2280.
- (61) Ramirez, F.; Dershowitz, S. The Structure of Quinone-Donor Adducts. I. The Action of Triphenylphosphine on p-Benzoquinone, 2,5-Dichloro-p-Benzoquinone and Chloranil. *J. Am. Chem. Soc.* **1956**, 78 (21), 5614–5622.
- (62) Song, N.; Gagliardi, C. J.; Binstead, R. A.; Zhang, M.-T.; Thorp, H.; Meyer, T. J. Role of Proton-Coupled Electron Transfer in the Redox Interconversion between Benzoquinone and Hydroquinone. J. Am. Chem. Soc. 2012, 134 (45), 18538–18541.
- (63) Arick, M. R.; Weissman, S. I. Direct Measurement of the Rate of Hydrogen-Atom Exchange between a Phenol and Its Phenoxy Radical. *I. Am. Chem. Soc.* **1968**, 90 (6), 1654–1654.
- (64) Huynh, M. T.; Anson, C. W.; Cavell, A. C.; Stahl, S. S.; Hammes-Schiffer, S. Quinone 1 e- and 2 e-/2 H+ Reduction Potentials: Identification and Analysis of Deviations from Systematic

- Scaling Relationships. J. Am. Chem. Soc. 2016, 138 (49), 15903-15910.
- (65) Gray, H. B.; Hendrickson, D. N.; Sohn, Y. S. Magnetic Susceptibility Study of Various Ferricenium and Iron(III) Dicarbollide Compounds. *Inorg. Chem.* **1971**, *10* (8), 1559–1563.